ON TURBULENCE AND TRANSPORT IN SHALLOW WAKE FLOWS

CARL F. V.CARMER & GERHARD H. JIRKA

Institute for Hydromechanics, University of Karlsruhe
Kaiserstr. 12, 76128 Karlsruhe, Germany
carmer@ifh.uni-karlsruhe.de

ABSTRACT

Natural flows can often be characterized as shallow turbulent shear flows. Due to local disturbances large coherent vortical structures are introduced in such base flows, and participate in the transport of momentum and mass. In order to gain more insight in the genesis and evolution of large-scale flow structures, the shallow flow around a single cylindrical obstacle was examined as a basic study in a turbulent vertical shear flow. Experiments were conducted in a shallow flow test facility applying an improved combined LDA-LIF measurement technique. Thus, coincident information was obtained about the horizontal velocity and scalar tracer with high temporal and spacial resolution. For shallow turbulent wake flows behind single cylindrical obstacles different instability types are presented differing significantly from unbounded wake flows. From the analysis of the 1D power spectral distributions the simultaneous occurance of large-scale 2D and small-scale 3D turbulent features in the flow is demonstrated as well as their interaction for different types of instability. The consequences of distinguishable turbulent scales are evidenced for the longitudinal evolution of turbulent kinetic energy, mass variance and longitudinal mass transport. The experimental data can be used to compute further characteristic measures for shallow wake flows. e.g. the energy and scalar dissipation rates. Because of the simple flow configuration and the well controlled boundary conditions, the data sets also provide a data base for the validation of numerical models, which are to be used in more complicated "real world" applications.

KEYWORDS

shallow wake flow, large coherent structures, large-/small-scale turbulence, LDA-LIF

INTRODUCTION

Turbulent shallow water flows having a limited vertical extend in a horizontally unbounded domain are ubiquitous in our environment, e.g. in wide rivers, lakes, estuaries, shallow coastal waters or the stratified atmosphere. Such base flows, which are sheared vertically at the fixed bottom (also at fluid-fluid interfaces), can be disturbed by large-scale instabilities, for example introduced from islands in a shallow water body. Large-scale eddy structures caused by such perturbations characterize the momentum and mass transport in the near-wake region. In a shallow domain a flow field can be recognized, which deviates significantly from flow structures in an unbounded ambient. On one hand, and purely kinematically, the reduced vertical dimension prevents a 3D decay by secondary transverse instabilities. On the other hand, from dynamical grounds, bottom friction effects lead either to a complete suppression of the generation of large structures at the obstacle or to a downstream re-stabilization of the wake flow.

The study of wake flows behind cylindrical bodies in shallow turbulent shear flow contributes to the understanding of the genesis and preservation principles of the associated large-scale eddy structures and helps to quantify their transport characteristics (for momentum, mass, and scalar tracers). Different instability mechanisms will be characterized regarding some of their

large- and small-scale flow characteristics. A complete representation of the physical phenomena was given by Chen & Jirka (1995). The first type of stability "VS" (Vortex Street) shows a formation, which resembles a von Karman vortex street, however with substantially larger cylinder Reynolds number Re_D (see Fig. 1). It is characterized by the alternating separation of large vortical structures directly from the cylinder shoulders. For another type of instability "UB" (Unsteady Bubble) the formation of a recirculation bubble occurs in the lee attached to the cylinder, from whose tail again alternating large eddies separate. In contrast to the VS type here the damping effect of the bottom friction is more dominating in relation to the production of turbulent kinetic energy due to horizontal shear, and vortex shedding at the cylinder perimeter is prevented. If the influence of the bottom friction is even more pronounced, or even less turbulent kinetic energy is extracted from the mean flow, the large-scale instabilities become completely suppressed. The formation of a stable recirculation bubble in the lee of the cylinder without any vortex shedding from ist tail is characteristic for a stability type "SB" (Steady Bubble) wake. Nevertheless, in this situation vortical structures from the lateral shear layers are introduced to the flow, which would also mature to large-scale 2D structures, if the shear layers would last long enough. As is shown below, there is some evidence for this mechanism, especially in more stable shallow wakes.

MEASURING TECHNIQUE AND EXPERIMENTAL SETUP

In order to examine the behavior of large-scale eddy structures in shallow turbulent shear flow, a large and well equipped shallow water test facility is available at the Institute for Hydromechanics, University of Karlsruhe. In that 5.50 m wide and 13.5 m long basin - operated at water depths of only a few centimeters - a plane turbulent equilibrium shear flow is produced by bottom friction working against the pressure gradient. In order to generate large-scale instabilities a horizontal shear flow (e.g. jets, wakes, free shear layers) could be superimposed to the vertical shear flow, or the base flow could be subjected to local or global deceleration (steady by expansion of the flow cross section, unsteady by discharge reduction). In the present study the disturbance is induced by the most intensive mechanism, namely a sudden local modification of the flow geometry. Here the base flow is forced to flow around a single cylindrical body with a diameter D, which is clearly larger than the water depth h.

For the analysis of the flow characteristics in shallow shear flow the substantial flow parameters are to be obtained in high temporal and spatial resolution both in their time history and in their relation For that purpose a combined non-invasive measurement technique was adapted and applied. With a 2-dimensional Laser Doppler Anemometer (LDA) powered by a continuous Argon-ion laser the horizontal velocity components are measured through the free water surface. In order to receive information about the mass transfer, small quantities of a fluorescent dye (Rhodamine B or Sulforhodamine B) are added continuously into the upstream cylinder boundary layers. The light backscattered from the LDA measuring volume

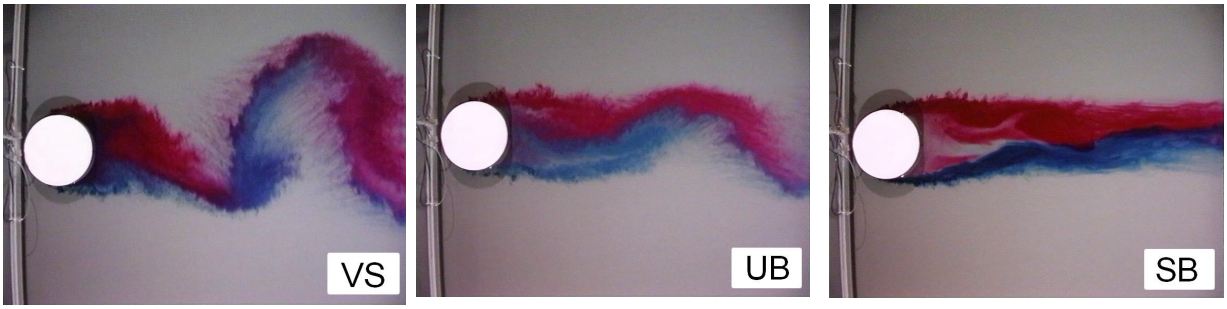

Fig. 1: Plane views of shallow wake instabilities of type "VS", "UB" and "SB", where cylinder diameter D = 430 mm, flow depth h = 30 / 20 / 11 mm, $Re_D = UD/\nu$ = 44.000 / 35.000 / 25.000, and $Re_h = Uh/\nu$ = 3.100 / 1.600 / 640, respectively

is subjected to a Laser Induced Fluorescence (LIF) analysis to obtain the local instantaneous concentration of the fluorescent dye. A complete synchronization of both measuring systems is obtained by storing simultaneously a voltage signal of the LIF to each LDA burst signal.

Contrary to the usual arrangements, the LIF system is operated in an on-axis backscatter mode. In order to resolve the highly dynamic concentration fluctuations in the given flow situation, the evaluable maximum concentration was increased around the factor 10 compared with the usual maximum concentrations. The non-linear relations between the extinction light intensity of the incident beams and detected emission intensity, which are associated with high dye concentrations for various reasons, were identified and quantified. For a detailled information see Carmer (2000). With an extended transfer function the absolute value of Rhodamine B concentrations up to 500 mg/m^3 can be determined reliably.

The measuring program consists of point measurements along the longitudinal axis in the wake of the cylinder. For each point data was sampled for 120 s or 600 s measuring periods with a mean data rate well over 100 s^{-1} per LDA channel, the stored data sets then were resampled equidistantly in coincident pairs with a data rate of 100 s^{-1}. Reference measurements in the ambient flow were conducted between the individual measuring points. The vertical position of the measuring volume was kept constant during each series of measurements at an elevation of about 2/3 of the water depth.

RESULTS

The evolution of the large-scale instabilities can be distiguished easily in the 1D power spectral density (psd) distributions, which show a very distinct peak in the near field of the cylinder perfectly in agreement with the natural frequency, corresponding for the VS type to a Strouhal number of 0.21 (see Fig. 2 for increasing distances x/D). Compared to the psd of the undisturbed ambient shear flow the whole low-frequency plateau, whereupon this peak is located, is lifted initially for about 2 decades above the ambient energy level. The energy contained in the low-frequency fluctuations decays with increasing x/D, without change of the wavenumber or the shape of the low-frequency peak. Transfer of mass and energy into still larger structures by vortex pairing can therefore be excluded. There only exists the cascading process associated with vortex stretching to small-scale structures and transition to the dissipation. At the same time the whole low-frequency energy content decreases, until the ambient energy level is approached. Comparing the different stability types it should be noted, that the width of the low-frequency peak increases when the large eddy structures become more stabilized, i.e. the frequency spectrum of the large-scale structures for the SB-type is wider than for the UB- or VS-type, and at the same time the production of turbulent kinetic energy decreases. Using a large structure scaling with the characteristic integral velocity and length scales of the eddies, this could be illustrated more clearly in the psd distributions.

Attention is also drawn to the fact, that the stability type UB compared to the VS type indicates as a characteristic feature, that the maximum value of the psd is not located directly behind the cylindrical body, but about 2 diameters downstream at x/D = 2. This corresponds to the end of the unsteady recirculation bubble. More important, the psd distributions for the type UB and SB instability show a wavenumber dependency, which, just above the peak number, obeys a -3 power law (see Fig. 2, left). This could also be ascribed to 2D vortical structures with length scales still larger than the water depth, which were also encountered in other shallow shear flows, e.g. in a plane shallow jet (Dracos, Giger & Jirka, 1992). In the same situation the psd of mass concentration follows a -1 power law, which is strikingly

obvious in all stability types from Fig. 2, right, for an even wider low-wavenumber range. For an analytical background of 2D turbulence the reader is referred to Lesieur (1997). Furthermore, all spectral features are of greater significance in the psd of the lateral velocity component than in the longitudinal. At a sufficiently large relative distance x/D from the obstacle, where the momentum defect is expected to vanish and the farfield to end, the ambient low-frequency energy level is approached. Nevertheless, the low-frequency peak can still be observed in the v-component psd, but not in the u-component (not shown in Fig. 2). In the corresponding autocovariance distributions for the u-velocity a complete decorrelation is found beyond a time associated with the integral time scale of the small-scale 3D background turbulence. Again for the same distance x/D the v-component still follows a periodic low-frequency behavior of large eddy structures.

Because of the relatively small Reynolds number in these experiments, the 1D power density spectra of the horizontal velocity components usually show just a short inertial range above the low-frequency production region, in which the -5/3 Kolmogorov power law of local-

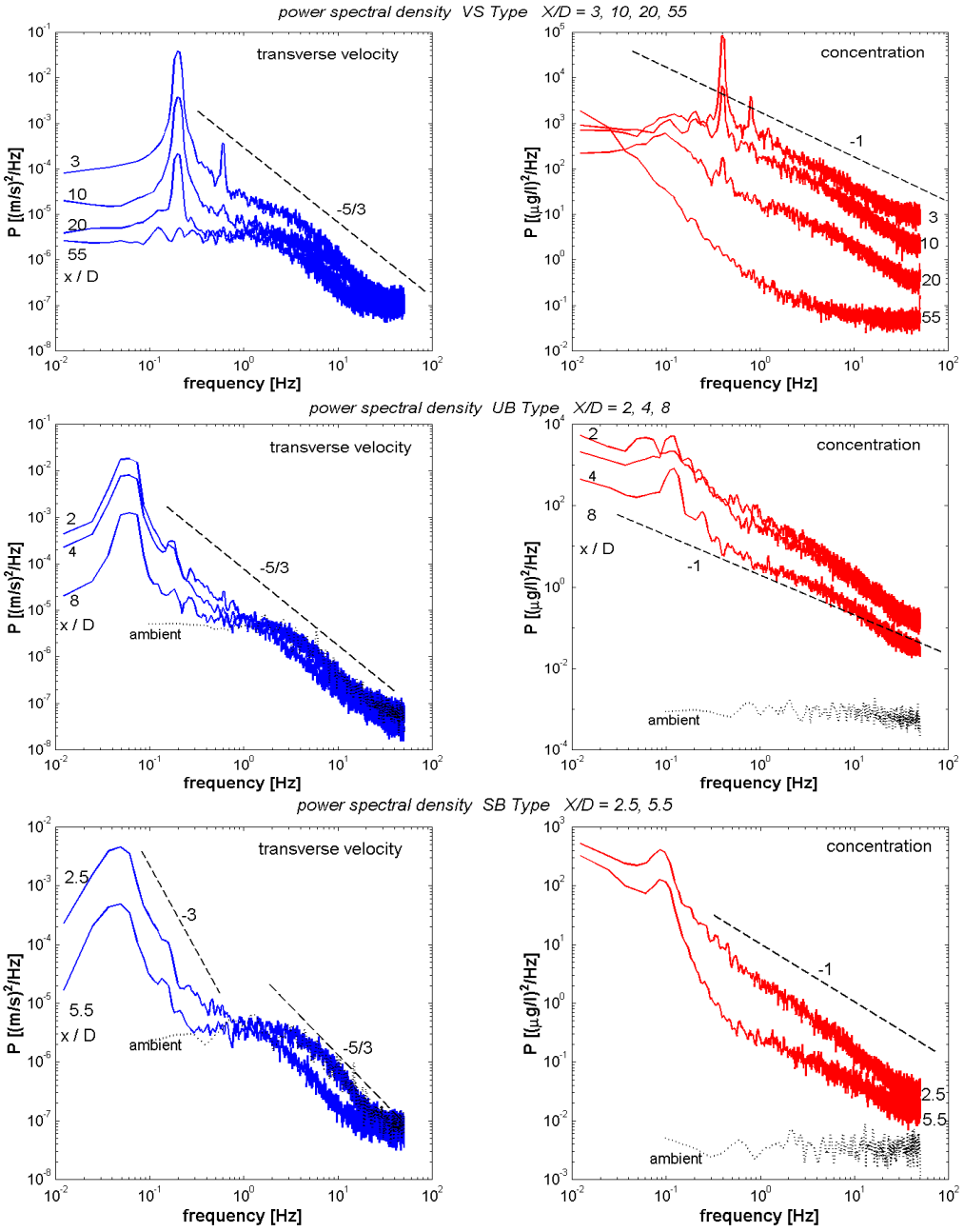

Fig. 2: 1D power spectral density distributions of transverse velocity v (left column) and mass concentration c (right column) for instability types VS, UB, SB (from top to bottom)

isotropic turbulence is applicable. Beyond that range the measurements resolve wavenumbers far into the viscous-dissipative range. A standardisation with the Kolmogorov microscales for length and velocity, i.e. with kinematic viscosity ν and dissipation rate ε, could still clarify this. For the mass concentration because of the large Schmidt number of the fluorescent dye we expect to find a clear viscous-convective range in the 1D power spectra of the concentration above the maximum wavenumber of the inertial range. In the large wavenumbers the well-known -1 power dependency on the wavenumber is clearly met over a long wavenumber range down to 2D turbulence behavior. Therefore, the 1D psd distributions of energy and mass refer to an inertial-convective range, in which the dissipation rates for energy and mass are constant.

A common triple-decomposition (eg. Hussain, 1983) of the velocity and concentration signals into steady-advective, large-scale coherent and small-scale-3D portions (e.g. $u = \langle u \rangle + u_c + u_r$ where angular brackets denote time averaging) was computed here by applying a low order curve fitting in a moving data window. This method to split up the data is rather simple, but effective for these phenomena, because it works on periodic low-frequency motions as well as on more random fluctuations occuring in SB-type instabilities. In the decomposed data it showed clearly (not presented here), that the high turbulence intensities in the near field have to be assigned to the large-scale structures, whereas the small-scale fluctuations are of the order of magnitude of the background turbulence. In order to determine the turbulent kinetic energy of the flow, it was thus assumed in the near field of the cylinder, that the contribution from the vertical (exclusively high frequency) fluctuations can be neglected with respect to the horizontal fluctuations. In the longitudinal development visualized in Fig. 3 the turbulent kinetic energy is normalized with the appropriate mean kinetic energy, thus the ratio $\left(\langle uu \rangle + \langle vv \rangle\right) \Big/ \left(\langle u \rangle^2 + \langle v \rangle^2\right)$ is presented here.

The energy decay starts with maximum values, which are 3 orders of magnitude above the level of the ambient flow, and follows a power dependency of the form $q^2 \propto x^n$ (eg. Zhou et al., 2000), where n is about 1.26. The background level is reached in the case of the VS instability after approximately 20 cylinder diameters, which is significantly faster than for unbounded cylinder wakes. Corresponding to the psd distribution the UB instability shows its maximum value of turbulent kinetic energy for x/D = 2, the re-stabilization of the flow occurs after about x_e = 10 D. For this momentum recovery distance the estimate $x_e/D = 2/S$, given by Chen & Jirka (1995) is confirmed, where S is a stability number, which is formed from the product of friction coefficient c_f and the geometrical shear ratio D/h. As mentioned above, although the momentum defect has recovered almost completely, a significant peak in the transverse velocity spectrum is still evident.

In contrast to the turbulent kinetic energy the total mass fluctuations show less variability in the mean flow direction. However, since low- and high-frequency mass fluctuations are of the same order of magnitude, the portion of the small-scale-3D mass fluctuations should not to be neglected. The maximum value of the normalized mass variance occurs both in the case of the VS

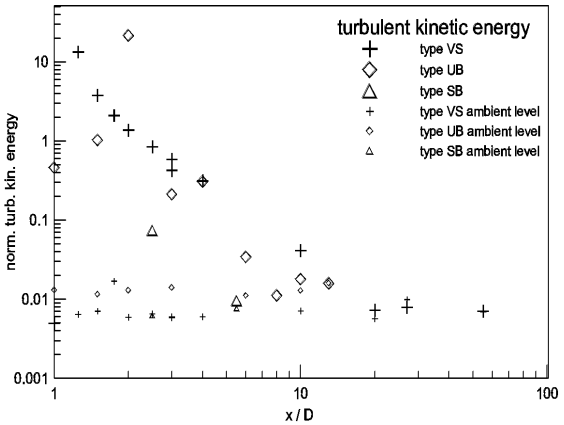

Fig. 3: Normalized turbulent kinetic energy

instability and for type UB after 4 cylinder diameters. When the turbulent kinetic energy is already completely extracted from the large-scale structures, the normalized mass variance amounts to still about 0.4. Further exchange of mass distribution in the flow field takes place only with the mechanisms of small-scale turbulent (and molecular) diffusion.

For the investigation of the mass flux in longitudinal direction again a triple-decomposition of the data can be applied, so that $\langle uc \rangle = \langle u \rangle \langle c \rangle + \langle u_c c_c \rangle + \langle u_r c_r \rangle + \langle u_c c_r \rangle + \langle u_r c_c \rangle$. It is found that in shallow cylinder wakes the dominating part of the longitudinal flux is allotted to the total of the steady-advective and large-scale coherent parts (first two terms on right hand side). The small-scale-3D portion (third term) is insignificant (< 1 % of total flux). Both cross-correlated fluctuation terms are of the same size, even decades smaller than the small-scale turbulent flux and therefore completely irrelevant for the total mass flux.

CONCLUSIONS

A large cylindrical obstacle introduced in a shallow turbulent vertical shear flow serves as a basic case for the evolution of large-scale instabilities in a shallow ambient with small-scale 3D turbulence. For this fundamental configuration the production and decay of turbulent kinetic energy induced in the large coherent structures is studied in the spectral and in the spatial domain. During the transfer of energy and mass to higher wavenumbers, there might co-exist a low-wavenumber region showing a 2D turbulence behavior besides an inertial-convective range in the higher wavenumbers revealing typical local-isotropic dependencies. From the longitudinal mass transport using the triple-decomposed data it can be concluded, that the small-scale fluctuations are of minor importance in the near-wake region and even in the far-wake.

More physical insight is needed in the fate of separate large coherent structures in shallow shear flow. Therefore in addition to pointwise measurements with high temporal resolution, a whole-field technique for velocity and mass will be employed in future work.

ACKNOWLEDGEMENTS

The support of the German Research Council (DFG Grant Ji 18/4-1) is acknowledged. CFvC would like to thank Chia R. Chu for helpful discussions on related topics.

REFERENCES

Antonia, R.A.; Mi, J. (1998): Approach towards self-preservation of turbulent cylinder and screen wakes. Exp. Thermal Fluid Sci., 17:277-284.

Carmer, C.F.v. (2000): LDA-LIF System zur Untersuchung großräumiger kohärenter Strukturen in flacher turbulenter Strömung. in: Delgado, A. et al. [Ed.]: Lasermethoden in der Strömungsmesstechnik. 8. GALA-Fachtagung. Shaker Verlag, Aachen.

Chen, D.; Jirka, G.H. (1995): Experimental study of plane turbulent wakes in a shallow water layer. Fluid Dyn. Res., 16:11-41.

Dracos, T.; Giger, M.; Jirka, G.H. (1992): Plane turbulent jets in a bounded fluid layer. J. Fluid Mech., 241:587-614.

Hussain, A.K.M.F. (1983): Coherent structures - reality and myth. Phys. Fluids, 26(10):2816-2850.

Lesieur, M. (1997): Turbulence in Fluids. Stochastic and Numerical Modelling. 3. rev. enlarged ed. Kluwer Academic Publishers, Dordrecht.

Warhaft, Z. (2000): Passive Scalars in Turbulent Flows. Ann. Rev. Fluid Mech., 32:203-240.

Zhou, T.; Antonia, R.A.; Danaila, L.; Anselmet, F. (2000): Transport equations for the mean energy and temperature dissipation rates in grid turbulence. Exp. Fluids, 28:143-151.